

Isospin diffusion in semi-peripheral $^{58}\text{Ni}+^{197}\text{Au}$ collisions at intermediate energies (I): Experimental results

E. Galichet,^{1,2,*} M. F. Rivet,¹ B. Borderie,¹ R. Bougault,³ A. Chbihi,⁴
R. Dayras,⁵ D. Durand,³ J.D. Frankland,⁴ D.C.R. Guinet,⁶ P.
Lautesse,⁶ N. Le Neindre,¹ O. Lopez,³ L. Manduci,³ M. Pârlog,⁷
E. Rosato,⁸ B. Tamain,³ E. Vient,³ C. Volant,⁵ and J.P. Wieleczko⁴

(INDRA Collaboration)

¹*Institut de Physique Nucléaire, Université Paris-Sud 11,
CNRS/IN2P3, F-91406 Orsay Cedex, France*

²*Conservatoire National des Arts et Métiers, F-75141 Paris Cedex 03, France*

³*LPC Caen, ENSICAEN, Université de Caen,
CNRS/IN2P3, F-14050 Caen Cedex, France*

⁴*GANIL, CEA et IN2P3-CNRS, B.P. 5027, F-14076 Caen Cedex, France*

⁵*IRFU/SPhN, CEA/Saclay, F-91191 Gif-sur-Yvette, France*

⁶*Institut de Physique Nucléaire, Université Claude Bernard Lyon 1,
CNRS/IN2P3, F-69622 Villeurbanne Cedex, France*

⁷*National Institute for Physics and Nuclear Engineering,
RO-76900 Bucharest-Măgurele, Romania*

⁸*Dipartimento di Scienze Fisiche e Sezione INFN,
Università di Napoli "Federico II", I-80126 Napoli, Italy*

(Dated: December 15, 2008)

Abstract

Isospin diffusion in semi-peripheral collisions is probed as a function of the dissipated energy by studying two systems $^{58}\text{Ni}+^{58}\text{Ni}$ and $^{58}\text{Ni}+^{197}\text{Au}$, over the incident energy range 52-74A MeV. A close examination of the multiplicities of light products in the forward part of phase space clearly shows an influence of the isospin of the target on the neutron richness of these products. A progressive isospin diffusion is observed when collisions become more central, in connection with the interaction time.

PACS numbers: 25.70.-z 25.70.mn 25.70.Kk

*Corresponding author: galichet@ipno.in2p3.fr

I. INTRODUCTION

The knowledge of the different time scales associated to the various degrees of freedom involved in heavy-ion collisions at intermediate energy is of crucial importance to determine the physical properties of nuclear sources produced (in the exit channel). Thermal equilibrium has been studied both theoretically and experimentally and times in the range 30-100 fm/c were derived in the Fermi energy region [1, 2, 3, 4, 5, 6]. With the announced exotic beams the N/Z degree of freedom will hopefully be explored over a wide range, and thus an estimate of the chemical (isospin) equilibration time becomes essential; moreover experimental constraints can be placed on the asymmetry term of the equation of state which describes its sensitivity to the difference between proton and neutron densities [7, 8, 9]. Theoretical simulations of collisions were performed using isospin-dependent Boltzmann-Uehling-Uhlenbeck transport equations [9, 10, 11]. In the energy domain 20-100A MeV, estimates of the chemical equilibration times in the range 40-100 fm/c are reported, if one excludes calculations with an asymmetry term rapidly increasing around normal density.

Experimentally some investigations concerning this time scale have been done. In the Fermi energy domain, studies on isospin equilibration in fusion-like reactions between medium nuclei ($A \sim 50$) have shown that isospin equilibrium occurred prior to light fragment emission, which gives an upper limit around 100 fm/c [12, 13]; for peripheral collisions between Sn isotopes [9] only a partial equilibrium (isospin asymmetry of the projectile remnant is half way between that of projectile and the equilibration value) is measured at the separation time (~ 100 fm/c) between quasi-projectile and quasi-target. At higher incident energy (400A MeV) the FOPI Collaboration measured the degree of isospin mixing between projectile and target nucleons, and found that complete mixing is not reached even in the most central collisions [14].

In the present study we concentrate on semi-peripheral collision measurements performed with the INDRA array. The properties of the de-excitation products of the quasi-projectiles inform on the degree of N/Z diffusion and the separation time between the two partners will be taken as a clock to derive qualitative information on isospin equilibration. Two reactions with the same projectile, ^{58}Ni , and two different targets (^{58}Ni and ^{197}Au) are used at incident energies of 52A MeV and 74A MeV. The N/Z ratios of the two systems are 1.07 for Ni+Ni and 1.38 for Ni+Au. INDRA only provides isotopic identification up to beryllium and

does not detect neutrons. Thus an N/Z ratio for complex particles is constructed which well reflects the evolution of the N/Z of quasi-projectiles with the violence of the collisions. (see the accompanying article [15]). The Ni+Ni symmetric system is taken as a reference since, on average, the isospin should remain constant with time whatever the collision process is.

The paper is divided into three sections. In a first part, we describe the experiment and the event selection, then we present the properties of quasi-projectiles and finally we discuss the evolution of the isospin, before concluding.

II. EXPERIMENT AND EVENT SELECTION

A. Experimental details

^{58}Ni projectiles accelerated to 52 and 74.4 MeV by the GANIL facility impinged on ^{58}Ni ($179 \mu\text{g}/\text{cm}^2$) and ^{197}Au ($200 \mu\text{g}/\text{cm}^2$) targets. The charged products emitted in collisions were collected by the 4π detection array INDRA. A detailed description of the apparatus can be found in references [16, 17, 18]. All elements were identified within one charge unit up to the projectile charge. Elements from H to Be were isotopically separated when their energy was high enough (above 3, 6, 8 MeV for p, d, t; 20-25 MeV for He isotopes; ~ 60 MeV for Li and ~ 80 MeV for Be). However isotopic identification was not possible in the first ring of INDRA, constituted of phoswiches, so in this paper the angular range is limited to $3\text{-}176^\circ$ for all products. In the following we shall call fragments the products for which only the atomic number is measured ($Z \geq 5$). The on-line trigger required that four modules of the array fired. The off-line analysis only considered events in which four charged products were identified.

The characteristics of the systems studied here are displayed in table I. Note that the grazing angle is below the minimum detection angle of INDRA (2°) for the Ni+Ni system at both energies. This shows through the lower measured percentage of the reaction cross sections ($\sigma_{M \geq 4}$, table I) for the Ni+Ni system (around 50%) as compared to those for the Ni+Au system (70%). The measured cross sections are derived from target thicknesses and integrated beam fluxes.

TABLE I: (color online) Characteristics of the systems studied : grazing angle, reaction cross section (calculated from [19]), and measured cross sections after the different selections

	Ni + Ni		Ni + Au	
	52	74	52	74
E_{inc}/A (MeV)	52	74	52	74
$E_{c.m.}$ (MeV)	1508	2146	2330	3316
θ_{gr} (lab)	1.9°	1.3°	4.6°	3.2°
σ_R (mb)	3460	3410	5400	5400
$\sigma_{M \geq 4}$ (mb)	1553	1634	3780	3807
Selected events (mb)	1032	953	3034	2885
Selected QP (mb)	624	491	904	793

B. Event selection

A first and simple selection required that the total detected charge amounts to at least 90% of the charge of the projectile. Figure 1 shows, for the two systems and the two energies, the location of the selected events in the total detected charge and momentum plane. In table I, one can observe that after this event selection, about 30% of the reaction cross section is kept for Ni+Ni, against 55% for the Ni+Au system: because of the detection geometry, peripheral collisions ($Z_{tot} \sim Z_{proj}$ and $P_{tot} \sim 1$) are drastically suppressed in the Ni+Ni reactions, neither the projectile nor the target remnants are detected. This effect exists but to a lesser extent for the very asymmetric Ni+Au system, thanks to the larger value of the grazing angle: here events with $Z_{tot} \sim Z_{proj}$ and $P_{tot} \sim 1$ are clearly visible. Conversely for this system the probability to detect all the products of an event ($Z_{tot} > 0.6$) is very small: the target-like fragment remains generally undetected because of the thresholds, unless it undergoes fission.

C. Selection of the quasi-projectile

A further selection must be done to select the “quasi-projectile”. We do not intend to isolate a “source”, but rather to select a forward region in phase space where the detected products have a small probability to result from emission by the quasi-target. In principle, this could be done by a cut at the center-of-mass velocity; for the asymmetric system

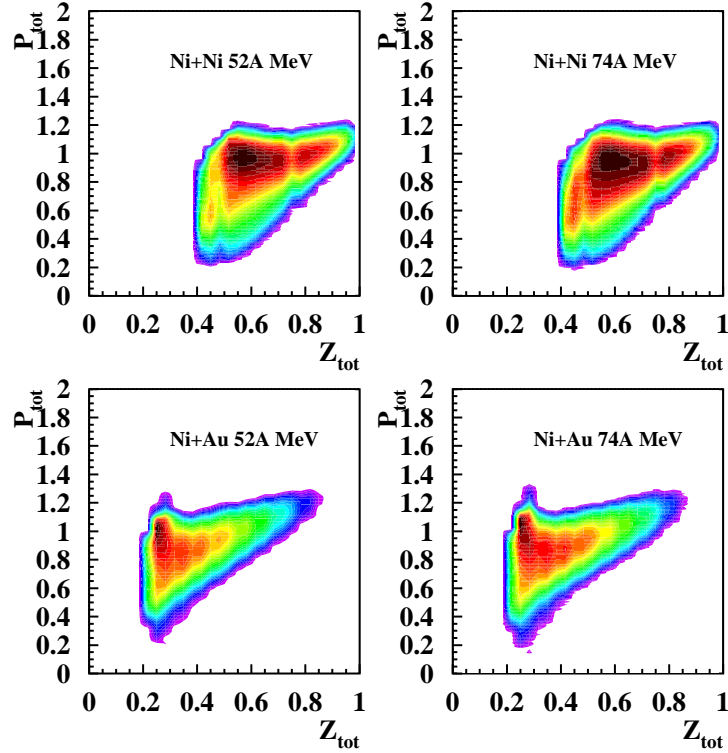


FIG. 1: (color online) The detected momentum P_{tot} versus the total charge Z_{tot} normalized to the incident momentum and the total charge of the system, for the Ni+Au and Ni+Ni systems at 52 and 74A MeV for the first selection. Event scale is logarithmic.

however, the target being more than three times heavier than the projectile, some particles from the target would be kept, as seen in fig. 2 which shows the charge of the products as a function of their laboratory velocity along the beam axis for the selected sets of events. Thus the cut was made at the nucleon-nucleon velocity - note that both cuts are identical for the Ni+Ni system. The quasi-projectile selection only keeps particles and fragments with a parallel velocity higher than the nucleon-nucleon velocity. It was verified that in this region of velocity space, all isotopes of H up to Be were fully identified (Z and A). In fig. 2 a small contribution of fragments which have a velocity $\sim 10\%$ smaller than the projectile velocity appears for the Ni+Ni reaction at 74A MeV incident energy. It was attributed to a beam halo interacting with the brass target holder and represents about 14% of the events [20]. In order to sharpen the comparison between quasi-projectiles produced in the two systems, the total charge beyond the nucleon-nucleon velocity was required to be in the range 24-32. In all cases 1.3 to 2×10^6 events are kept, amounting to 14-18% of the reaction cross sections.

In short in the following we call “quasi-projectile” the ensemble of charged products

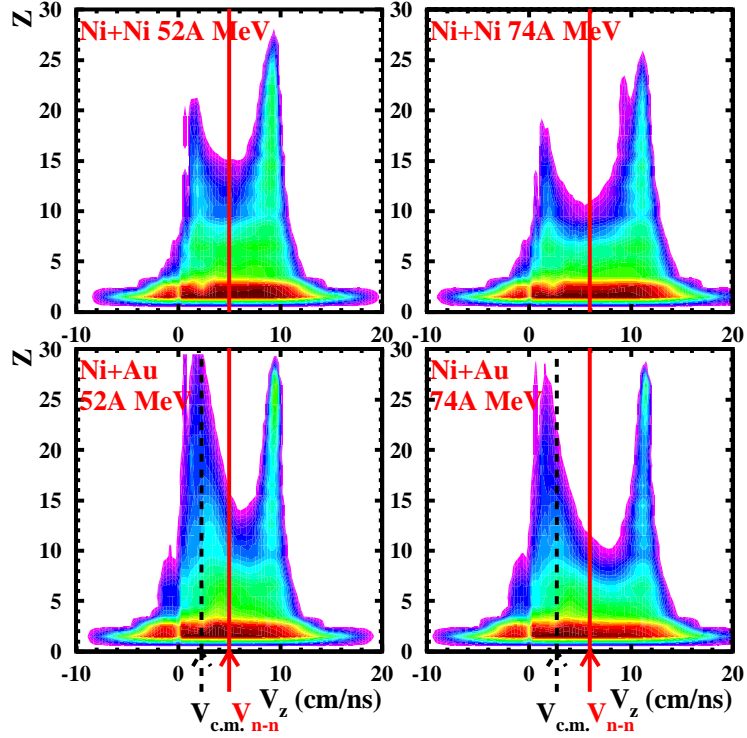


FIG. 2: (color online) The emitted products, for the selected events, in $Z - V_Z$ plane for the Ni+Ni and Ni+Au systems at 52 and 74A MeV. V_Z is in the laboratory system.

which have a velocity higher than the nucleon-nucleon velocity, without prejudice on the shape, degree of equilibration ... of the ensemble so defined. In figure 3 is represented the fragment ($Z \geq 5$) multiplicity distribution after all selections. In all cases a majority of the quasi-projectiles have only one fragment, which can be considered as the quasi-projectile remnant. For the Ni+Ni system, about 25-30% of the events have two or more fragments while for the Ni+Au system this percentage is smaller ($\sim 15\%$).

III. PROPERTIES OF THE QUASI-PROJECTILES

A. Event sorting

The method consisting in doing a calorimetry from the measured products can not be applied here, because it would require firstly to isolate sources and secondly an assumption on the number of neutrons, and thus on the N/Z of the quasi-projectiles, which is just the quantity we want to work out. To avoid the above difficulties we choose to sort the events as

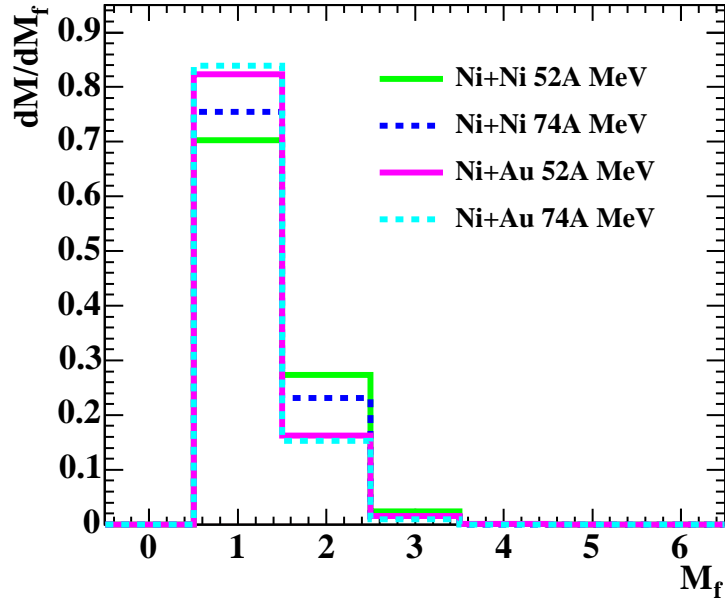


FIG. 3: (color online) Multiplicity distribution for fragments, $Z \geq 5$, for the selected quasi-projectiles.

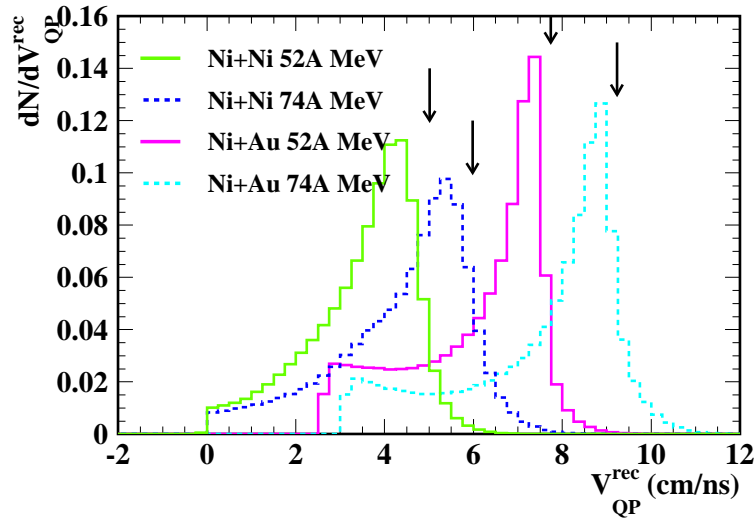


FIG. 4: (color online) Reconstructed velocity of the quasi-projectile in the center of mass frame for the two systems and the two energies. The arrows indicate the projectile velocity.

a function of the dissipated energy, calculated in a binary hypothesis, with the assumptions detailed below.

i) The quasi-projectile velocity is equal to the measured velocity of the fragment, or reconstructed from the velocity of all the fragments it contains. The distribution of the quasi-

projectile velocities (V_{QP}^{rec}) so determined are represented, in the center-of-mass reference frame, on figure 4. In all cases the reconstructed velocity of the quasi-projectile peaks at a value smaller than the projectile velocity, but remains closer to it for the Ni+Au system.

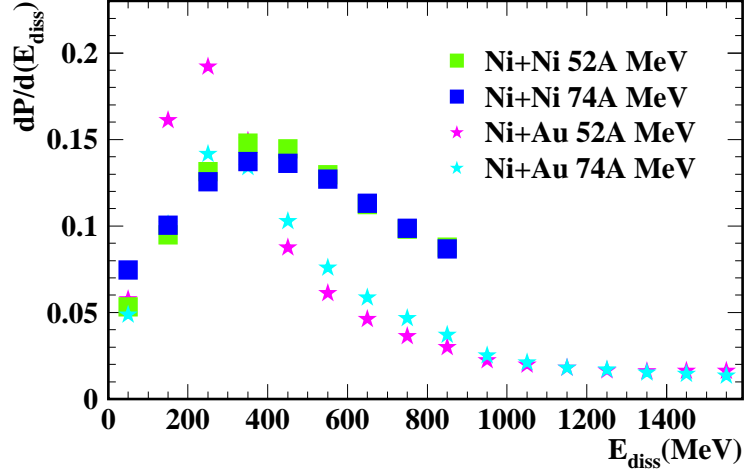


FIG. 5: (color online) Distributions of the dissipated energy for Ni+Ni and Ni+Au at 52 and 74 A MeV.

ii) The relative velocity between the quasi-projectile and the quasi-target is determined as if the collision was purely binary, without mass exchange:

$$V_{rel} = V_{QP}^{rec} \times \frac{A_{tot}}{A_{target}} \quad (1)$$

and thus the total dissipated energy reads:

$$E_{diss} = E_{c.m.} - \frac{1}{2}\mu V_{rel}^2, \quad (2)$$

with μ the initial reduced mass. It is demonstrated in [21, 29] that the velocity of the QP is a good parameter for following the dissipated energy, except in very peripheral collisions, due to trigger conditions. Moreover, it is shown in figure 5 of the accompanying paper that E_{diss} gives a good measure of the impact parameter.

In figure 5 are represented the dissipated energy distributions. For the Ni+Ni system and at the two incident energies, the distributions present a maximum at $E_{diss} \approx 350$ MeV, while they peak at lower dissipated energies for Ni+Au. This was expected from the remarks made in the previous sections; the most peripheral collisions - low excitation energies - are much more poorly sampled for Ni+Ni reactions than for Ni+Au. The comparison of the

properties of the quasi-projectiles between the two systems will be made by sorting data in bins of 100 MeV dissipated energy.

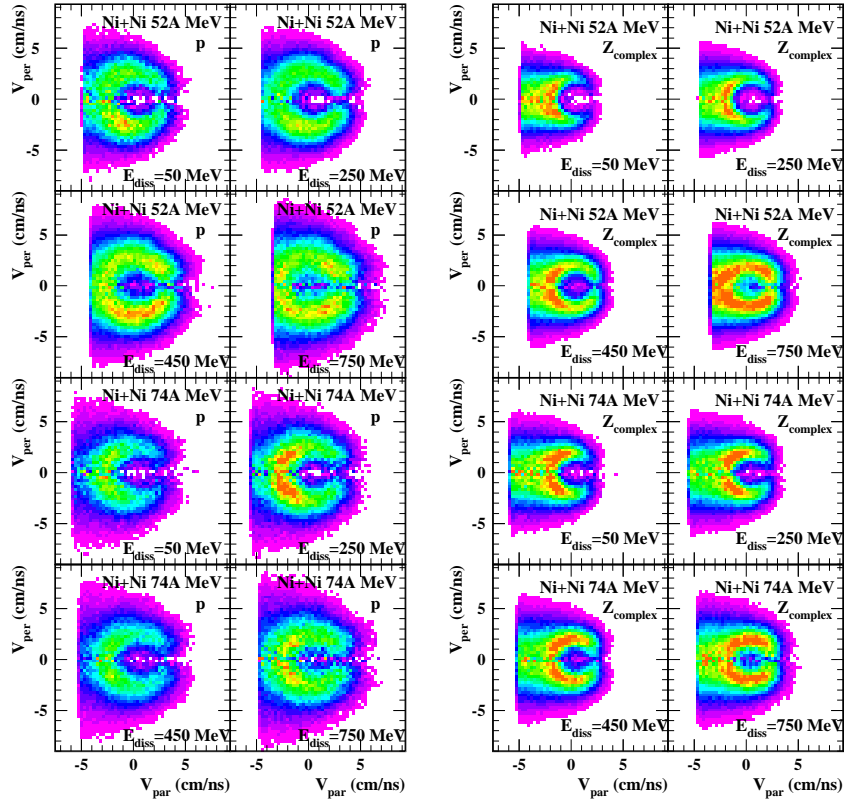


FIG. 6: (color online) Invariant cross sections for protons (left) and complex particles (right) emitted in the Ni+Ni system at 52 and 74A MeV. Velocities are expressed in the quasi-projectile frame. Contour levels are equidistant.

B. Invariant cross-section plots

As a verification of the selections and sorting made, we examined the repartition of the different particles in the velocity plane. A sign has been attributed to the perpendicular velocity depending on the value of the azimuthal angle ($V_{per} < 0$ corresponds to azimuthal angles larger than 180°). Such plots in the lab system allow a rough verification of the good operation of the INDRA array. Figs. 6, 7 are presented in the QP frame. The observed asymmetry between positive and negative values of V_{per} comes from a deviation of the beam position from the symmetry axis of INDRA, reflected in the azimuthal distribution

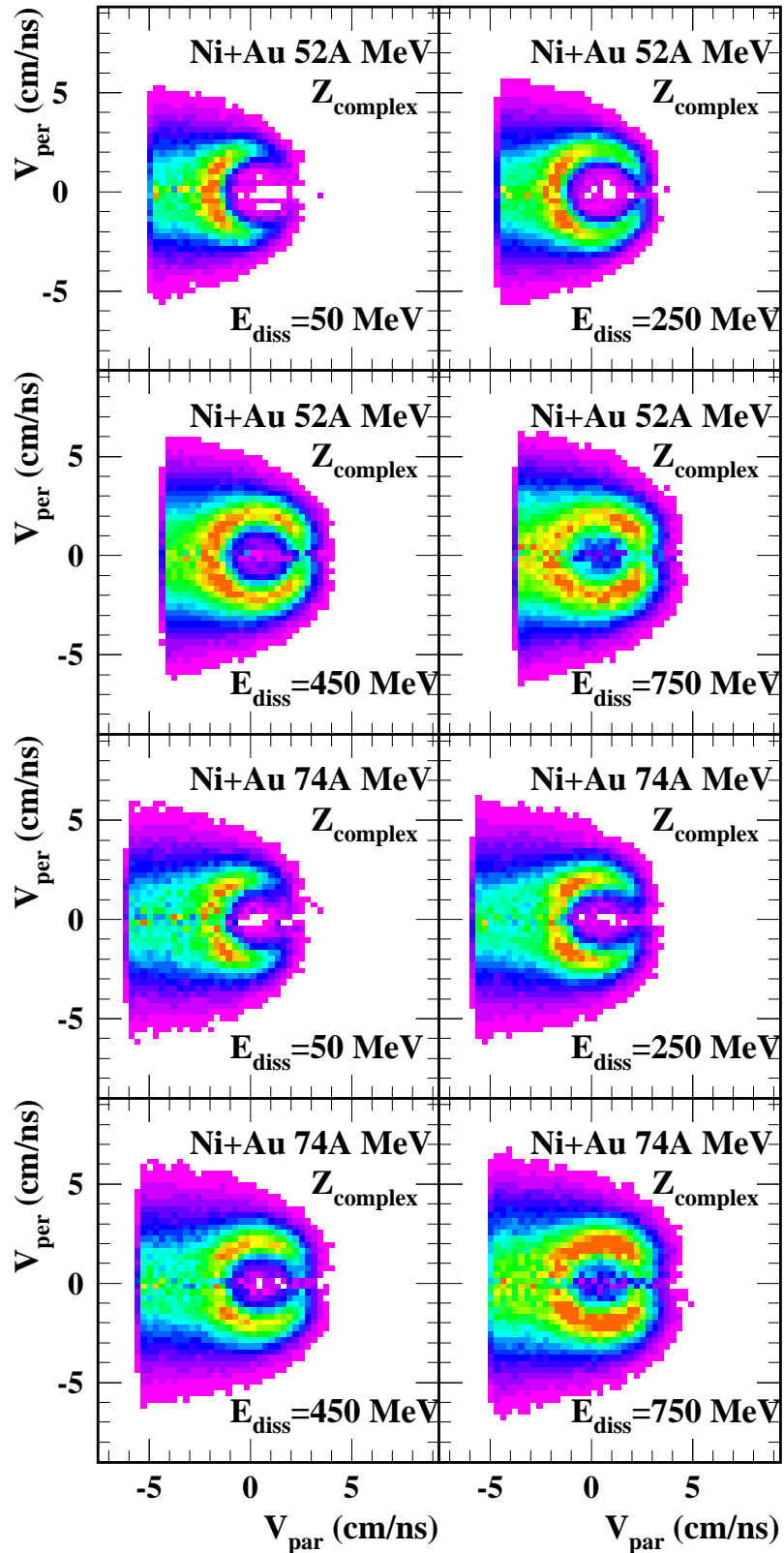


FIG. 7: (color online) Invariant cross sections of complex particles emitted in Ni on Au collisions at 52 and 74A MeV.

of projectile residues, and thus showing up when transforming all particles in the frame of this fragment. This is particularly visible for protons at 52A MeV in fig. 6, and does not affect the following results. In the left panel of figure 6 the invariant cross sections for protons emitted in the Ni+Ni reactions are presented. For all bins of dissipated energy and for the two incident energies, well-defined Coulomb circles are visible, showing that the protons essentially come from one source. The mid-rapidity/neck emission does not seem to be prominent at 52A MeV, except at low dissipation, (due to the online trigger, when QP and QT are too little excited for evaporating charged particles, configurations with several mid-rapidity particles are enhanced) while it becomes more important for all dissipations at 74A MeV. Due to the smaller quasi-projectile velocity at 52A MeV, and to the large proton velocities, the Coulomb circles are slightly cut at the higher dissipated energies (upper pannel). On the right panel of figure 6 are displayed the same plots for complex particles, including deuterons, tritons, helium, lithium and beryllium isotopes and labelled $Z_{complex}$ in figures 6 and 7. The Coulomb circles are also clearly visible, but an accumulation of particles appears backwards of the quasi-projectile due to the importance of mid-rapidity emission for such products; for the highest dissipated energies the distributions become more forward/backward symmetric for particles emitted at the Coulomb velocity. No sizeable emission from the target is present.

For protons emitted in Ni+Au collisions, the pictures (not shown) resemble closely those for Ni+Ni at the same incident energy. In figure 7 are represented the same pictures for complex particles for the Ni+Au system. As in the Ni+Ni system neck emission is apparent at low dissipation and Coulomb rings become more symmetric for higher dissipated energies in all cases.

C. The heaviest fragment

Figure 8 represents the charge distribution of the heaviest fragment ($Z \geq 5$) of the quasi-projectile, for the four reactions in each dissipated energy bin. For the Ni+Au system, the heaviest quasi-projectile fragment has a charge around $Z_{max}=24$ for peripheral collisions ($E_{diss} < 450$ MeV). These events have a quasi-projectile fragment multiplicity of one. In all other cases for this system there is no privileged value of the maximum charge, they often correspond to quasi-projectiles with more than one fragment. Note that the Z_{max}

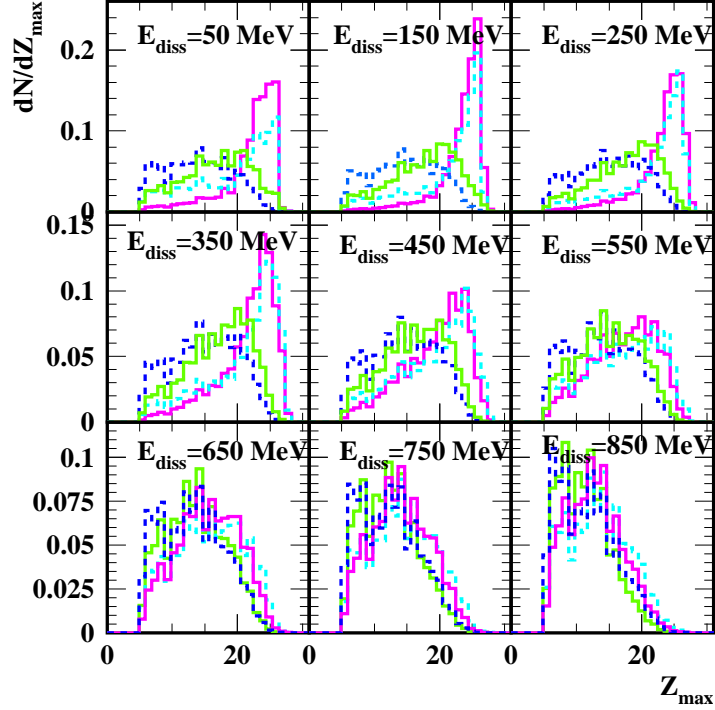


FIG. 8: (color online) Distribution of the heaviest quasi-projectile fragment for the four systems. The line codes are the same as in fig. 4

distributions barely depend on the target or on the energy when the dissipated energy overcomes 600 MeV.

For the Ni+Ni system, the distributions of Z_{max} do not exhibit any peak whatever the dissipation, which again agrees with the lack of very peripheral collisions in the event samples.

D. Multiplicity of particles

The average multiplicities of isotopically resolved charged products associated with quasi-projectiles for each energy bin are displayed in figure 9.

Let us first examine the Ni+Ni system. For hydrogen isotopes the multiplicity is constant at low energies and then rises. For other products the multiplicity slightly decreases before rising with the dissipated energy, above 400-500 MeV. It is indeed at this value that the dissipated energy distribution of the selected quasi-projectiles shows a maximum (fig 5). The effect is more marked for the heavier products; indeed for the most peripheral collisions,

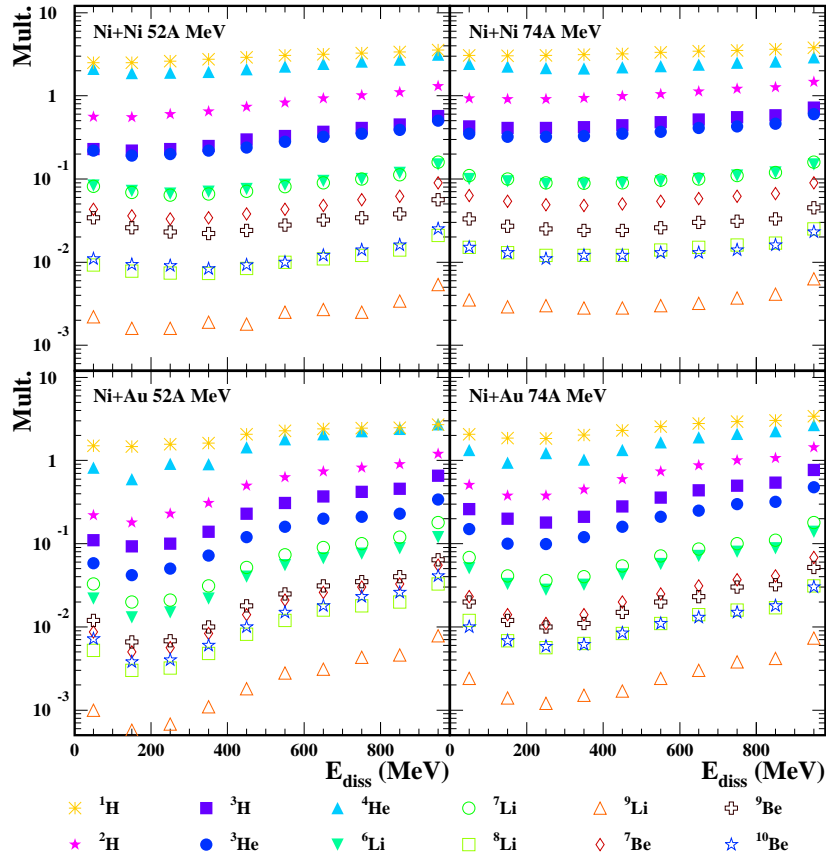


FIG. 9: (color online) Multiplicity of emitted products ($Z < 5$) versus the dissipated energy. In all cases, statistical error bars are smaller than the size of the symbols

due to the on-line trigger (4 detected charged products), some particular configurations were retained namely those with the highest multiplicities. A situation sampling all configurations for a given dissipation is recovered when the multiplicities start to increase. At 52A MeV the ratio between the maximum and the minimum values of the multiplicities is around 1.5 for protons and α particles, and more than 2.5 for other products. At 74A MeV, the observed multiplicities are generally close to those for 52A MeV. Systematically higher values are however found at lower dissipated energies (< 400 MeV) and in all cases for neutron rich hydrogen and lithium. This obviously comes from the sorting parameter which is not the excitation energy of an equilibrated piece of matter. At the higher energy the ratios between the maximum and the minimum values of the multiplicity of any species are smaller than at 52A MeV.

For the Ni+Au system the multiplicity variations closely resemble those of the Ni+Ni

case, showing firstly a slight decrease before a neat increase above dissipations of 250 MeV, which also corresponds to the peak in the dissipated energy distribution (see fig. 5). At both incident energies the ratios between the maximum and the minimum values of the multiplicity of any species are much higher than in the corresponding Ni+Ni case, particularly for lithium and beryllium isotopes (ratios as high as 10 are observed). The multiplicities for neutron rich species are smaller at 74 than at 52A MeV, showing the reverse evolution with respect with the Ni+Ni data. If one now compares the different multiplicities for Ni+Ni and Ni+Au, several differences immediately appear from fig 9: for Ni+Au, there are twice more protons than α 's at low dissipated energy, while both multiplicities tend towards equal values with increasing dissipation. Conversely the difference between proton and α multiplicities is almost constant around 30 (40)% for Ni+Ni at 52 (74)A MeV. For the Ni+Au system, all neutron rich isotopes are more abundantly produced, as can be seen by comparing tritons and ^3He , ^6Li and ^7Li , ^7Li and ^7Be , ^7Be and ^9Be . A simple way of observing the isospin effect is to calculate the average mass per element for the two systems, starting from figure 9. As expected, and due to the huge dominance of α 's, the average mass of helium is insensitive to the isospin of the target at variance to those of hydrogen, lithium and beryllium which increase with the target neutron excess. These observations indicate that there is a transfer of neutrons, or an isospin diffusion, from the backward to the forward part of phase space. Similar observations were made for vaporised silicon quasi-projectiles after interaction with targets with different isospins [22]; as in this paper, we also notice, from the evolution of the average element masses, that hydrogen and beryllium are more sensitive to the isospin of the target than lithium. The average masses are however insensitive to the dissipation, except a slight increase observed for hydrogen in Ni+Au data. A combination of the multiplicities of the different light isotopes will therefore bring more information than the individual evolution per element. The authors of [23] also noted a decrease of the $t/{}^3\text{He}$ ratio at low temperature, as predicted by Lattice Gas Model calculations [24]. In the present data the evolution of this ratio with excitation is weak but follows the same trend.

To summarize this part, a close examination of the multiplicities of light products in the forward part of phase space clearly shows an influence of the isospin of the target on the neutron richness of these products. In other words there is an isospin diffusion from the target side to the projectile side in the course of the reaction. This effect will be quantified by a single variable in the next section.

IV. ISOSPIN DIFFUSION AND EQUILIBRATION

A. Isospin ratio of complex particles

The isospin ratio of quasi-projectiles in intermediate energy heavy ion collision was abundantly studied in the 80's, when the first beams at these energies appeared. The underlying idea was already the determination of the equilibration time of the isospin degree of freedom. The reactions involved ^{40}Ar and $^{84,86}\text{Kr}$ projectiles at 27-30 and 44A MeV (see [25] and references therein for a review). The average N/Z were determined from Z=5 up to the projectile charge, at very forward angles, thus for very small dissipation; to our knowledge, no attempt to study the evolution of N/Z as a function of the dissipated energy, as proposed in the present paper, was ever made. For a given projectile and bombarding energy, it was found that the average N/Z of residues increases with the target N/Z. The difference between a ^{58}Ni and a Au target becomes smaller when the incident energy increases. Indeed the average N/Z tends towards that of the valley of stability, because of increasing dominance of the de-excitation process. This indicates that to characterize the primary process, not only the projectile residue (Z_{max} in this paper), but also all the emitted products should be detected, including neutrons. No data ever reached this ultimate goal. More information should however be extracted from the emitted products than from Z_{max} . In the experiments discussed here, INDRA only provides isotopic identification for isotopes of hydrogen up to beryllium and moreover does not detect neutrons. We wanted to avoid any hypothesis on heavy fragment masses and on the number of emitted neutrons, which would bias our conclusions; we thus construct an isospin ratio for complex particles, most probably different from the (N/Z) of the quasi-projectile, but evolving in the same way with increasing dissipation, as it is shown in the joint paper [15]. This variable, $(\langle N \rangle / \langle Z \rangle)_{CP}$, is calculated for each dissipated energy bin (containing N_{evts} events) and is defined as

$$(\langle N \rangle / \langle Z \rangle)_{CP} = \sum_{N_{evts}} \sum_{\nu} N_{\nu} / \sum_{N_{evts}} \sum_{\nu} P_{\nu} \quad (3)$$

where N_{ν} and P_{ν} are respectively the numbers of neutrons and protons bound in particle ν , ν being d, t, ^3He , ^4He , ^6He , ^6Li , ^7Li , ^8Li , ^9Li , ^7Be , ^9Be , ^{10}Be ; free protons are excluded as well as ^8Be , the latter because they are only partly identified, when the two α 's that they emit hit the same scintillator. The relative abundances of these nuclei among all those

emitted by the quasi-projectiles are assumed to reflect the isospin of the initial emitter. We recall that the light nuclei included in eq. 3 are fully identified, without any energy threshold. Relative systematic errors on $(\langle N \rangle / \langle Z \rangle)_{CP}$ as a function of dissipation mainly come from the wrong identification of a ${}^8\text{Be}$ as two α 's; they are lower than 0.4%.

B. Evolution of isospin with centrality

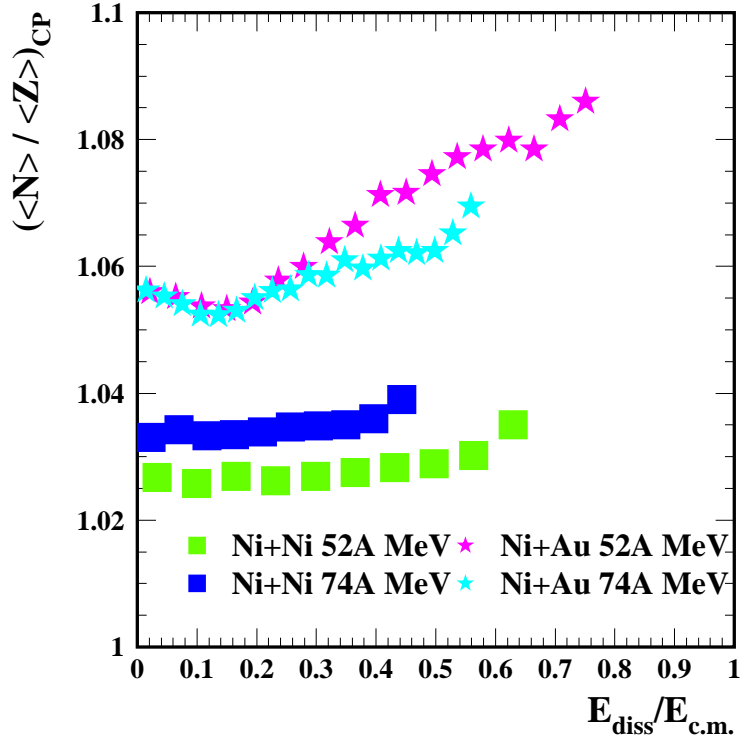


FIG. 10: (color online) Isospin ratio for complex particles as a function of the normalised dissipated energy. Statistical error bars are smaller than the size of the symbols.

In figure 10 the N/Z ratio for complex particles is plotted as a function of the normalised dissipated energy for the four reactions. The stars correspond to the Ni+Au system and the squares to the Ni+Ni system. We stress again that errors are very small, and thus the observed variations are significant. It immediately appears from the figures that the behaviour of $(\langle N \rangle / \langle Z \rangle)_{CP}$ is completely different for the two systems.

Let us first examine the Ni+Ni data. Within about 1.5% $(\langle N \rangle / \langle Z \rangle)_{CP}$ values are independent of the dissipated energy, at 52 and 74A MeV; this can be interpreted as the sign that the variable, used as reference, well reflects the evolution of the average isospin

of the initial quasi-projectiles, which is expected to be constant for this system, provided that the de-excitation process does not influence the isospin ratio. The observed value of $(\langle N \rangle / \langle Z \rangle)_{CP}$, closer to 1 than the N/Z of the system (1.07), comes from the dominance of α 's among the particles used to calculate it. Moreover $(\langle N \rangle / \langle Z \rangle)_{CP}$ is little dependent on the incident energy. The slight difference observed must be attributed to direct particles emitted at mid-rapidity or neck effect, which are included in the calculation of $(\langle N \rangle / \langle Z \rangle)_{CP}$. Another explanation may be that the system is proton rich, which favors proton preequilibrium emission; preequilibrium emission is expected to increase with the incident energy leading to an increase of the N/Z of primary quasi-projectile (target). This effect is observed in the isospin ratio, independently of the dissipation as the system is expected to remain, on average, symmetric. Observing such an effect is an indication that the chosen variable is indeed sensitive to the initial N/Z of the quasi-projectile.

Let us turn now to Ni+Au. A first observation is that the isospin ratio of the Ni+Au system is higher than the isospin ratio of the Ni+Ni system whatever the dissipated energy. One may argue that the difference of $(\langle N \rangle / \langle Z \rangle)_{CP}$ between the two systems is small (0.02-0.05, compared to 0.31 for the true N/Z values for the composite systems). This again can be attributed to the definition of the variable, built on particles among which deuterons and α 's are dominant. Therefore $(\langle N \rangle / \langle Z \rangle)_{CP}$ remains closer to 1 than the true isospin of the quasi-projectiles, the larger excess of neutrons being evacuated by free neutrons. The heavy fragments do not carry away a lot of neutrons : it was shown in [26] that for a given projectile, the $\langle N \rangle / Z$ of the heavy fragments are more neutron rich with a Au target than with a Ni target: the difference in average N/Z for ^{40}Ar residues is about 0.02-0.03, namely the same as what is observed here. Owing to these effects, we think that the gap between the values of $(\langle N \rangle / \langle Z \rangle)_{CP}$ for the two systems is significant and the mixing with the Au target did occur. Hence our variable well reflects the isospin diffusion between the target and the projectile as it is confirmed by figure 8 of the joint paper [15] where one can see that $(\langle N \rangle / \langle Z \rangle)_{CP}$ values change as those of N/Z for quasi-projectiles but within a reduced and lower domain. For the three first bins of dissipated energy $(\langle N \rangle / \langle Z \rangle)_{CP}$ has the same value for the two incident energies and slightly decrease with dissipation. These points should however be regarded with caution, they correspond to the region where multiplicities decrease with increasing dissipation, due to the selection of particular configurations by the on-line trigger. The isospin ratio of the Ni+Au system is however higher than that of

the Ni+Ni system, which could arise from the neutron skin of the Au target and/or from the mid-rapidity particles included in our quasi-projectile selection which are more neutron rich [27, 28]. This result is a first indication of isospin diffusion.

At higher dissipated energies, $(\langle N \rangle / \langle Z \rangle)_{CP}$ behaves differently depending on the incident energy. While $(\langle N \rangle / \langle Z \rangle)_{CP}$ presents a significant increase with dissipation at 52A MeV, the trend is flatter at 74A MeV. $(\langle N \rangle / \langle Z \rangle)_{CP}$ thus reaches higher values at 52A MeV. This may be interpreted as a progressive isospin diffusion when collisions become more central, in connection with the interaction time. For a given centrality, the separation time is longer at 52A MeV than at 74A MeV, leaving more time to the two main partners to go towards isospin equilibration.

V. CONCLUSION

To summarize, the value of the isospin variable $(\langle N \rangle / \langle Z \rangle)_{CP}$ for Ni+Au is different from and larger than that for Ni+Ni. It does not significantly evolve for the Ni+Ni system, neither with the excitation energy, nor with the incident energy when increased from 52 to 74A MeV. Therefore $(\langle N \rangle / \langle Z \rangle)_{CP}$ for Ni+Ni provides a good reference to which the same variable for Ni+Au can be compared. The continuous increase of $(\langle N \rangle / \langle Z \rangle)_{CP}$ up to the highest observed dissipation for Ni+Au at 52A MeV indicates that at least a partial isospin equilibration is reached at the corresponding separation time, ~ 80 fm/c. The separation time t_{sep} was estimated by $t_{sep} \sim (D_{Ni} + D_{Au} + d) / v_{beam} \sim 80$ fm/c at 52A MeV and 66 fm/c at 74A MeV; D is the nuclear diameter, v_{beam} the incident velocity and $d=3$ fm the distance between the two nuclear surfaces at separation.

We will see in the accompanying article [15] that, in the framework of the model employed, $(\langle N \rangle / \langle Z \rangle)_{CP}$ gives a reliable picture of isospin diffusion in the reactions studied and is relevant to determine if isospin equilibration takes place or not for the high excitation energies.

-
- [1] G. F. Bertsch, Z. Phys. A 289 (1978) 103.
 - [2] C. Toepffer et al., Phys. Rev. C25 (1982) 1010.
 - [3] W. Cassing, Z. Phys. A 327 (1987) 447.

- [4] C. Grégoire et al., Nucl. Phys. A 465 (1987) 317.
- [5] W. Rosch et al., Nucl. Phys. A 496 (1989) 141.
- [6] B. Borderie et al., Z. Phys. A - Hadrons and Nuclei A 357 (1997) 7.
- [7] B. Li et al., Isospin physics in heavy-ion collisions at intermediate energies, Nova Science, Huntington, New-York, 2001.
- [8] V. Baran et al., Nucl. Phys. A 703 (2002) 603.
- [9] M. B. Tsang et al., Phys. Rev. Lett. 92 (2004) 062701.
- [10] Bao-An Li et al., Int. Journ. of Mod. Phys. E 7 (1998) 147.
- [11] L. Shi et al., Phys. Rev. C 68 (2003) 064604.
- [12] H. Johnston et al., Phys. Lett. B371 (1996) 186.
- [13] H. Johnston et al., Phys. Rev. C56 (1997) 1972.
- [14] F. Rami et al., Phys. Rev. Lett. 84 (2000) 1120.
- [15] E. Galichet et al., accompanying paper.
- [16] J. Pouthas et al., Nucl. Inst. and Meth. A 357 (1995) 418.
- [17] J. Pouthas et al., Nucl. Inst. and Meth. A 369 (1996) 222.
- [18] J. C. Steckmeyer et al., Nucl. Inst. and Meth. A361 (1995) 472.
- [19] S. Kox et al., Nucl. Phys. A420 (1984) 162.
- [20] J. Guy et al., internal INDRA report.
- [21] R. Yanez et al., Phys. Rev C 68 (2003) 011602.
- [22] M. Veselsky et al., Phys. Rev. C 62 (2000) 064613.
- [23] M. Veselsky et al., Phys. Rev. C 62 (2000) 041605.
- [24] P. Chomaz et al., Nucl. Phys. A 647 (1999) 153.
- [25] B. Borderie et al., Ann. Phys. Fr. 15 (1990) 287.
- [26] R. Dayras et al., Nucl. Phys. A 460 (1986) 299.
- [27] T. Lefort et al. (INDRA Collaboration), Nucl. Phys. A 662 (2000) 397.
- [28] E. Plagnol et al. (INDRA Collaboration), Phys. Rev. C 61 (1999) 014606.
- [29] S. Piantelli et al., Phys. Rev. C 74 034609 (2006).